Radiative Muon Capture in Ca⁴⁰ and the Induced Pseudoscalar Coupling Constant

M. Conversi,* R. Diebold,† and L. di Lella

CERN, Geneva, Switzerland

(Received 10 July 1964)

The process $\mu^- + p \rightarrow n + \nu + \gamma$, where p is a proton in Ca⁴⁰, was observed by detecting the γ ray in a large NaI crystal. Only that part of the γ-ray spectrum lying above 60 MeV was analyzable because of large backgrounds at lower energies. The γ-ray spectrum is predicted theoretically to be rather sensitive to the value of g_P, the induced pseudoscalar coupling constant. Under the assumption that the pseudoscalar terms are induced by one-pion intermediate states only, the results of the experiment, as interpreted with the theory of Rood and Tolhoek, indicate that $g_P = (13.3 \pm 2.7)g_A$, where g_A is the axial vector coupling constant, and the error does not include the uncertainty in the theory. This value is two standard deviations larger than the predicted value of (7 or 8)g_A. The discrepancy may be statistical or the result of inadequacies in the theory describing the process. Alternative explanations can also be found. For example, one can assume that there actually is an excess Δg_P above that expected; assuming this excess to be independent of q^2 ($q =$ four-momentum transfer) our data give $\Delta g_P = (10.4 \pm 5.6)g_A$. Another possible explanation would be to drop the usual assumption that the weak currents have a definite transformation character under G parity, so that a tensor term (with $g_T \gtrsim 15g_V$) appears in the axial vector part of the weak current. Using the theory to extrapolate the γ-ray spectrum to low energies, a value of $(3.1 \pm 0.6) \times 10^{-4}$ was obtained for the ratio of radiative to ordinary muon capture. It was found that the average excitation energy given to the K⁴⁰ nucleus is (15 ± 4) MeV.

I. INTRODUCTION

THE weak interaction processes of β decay,

$$n \rightarrow p + e^- + \bar{\nu}_e, \tag{1}$$

and muon decay,

$$\mu^+ \rightarrow e^+ + \nu_e + \bar{\nu}_\mu, \tag{2}$$

have been extensively studied and are rather well understood.

On the other hand, muon capture,

$$\mu^- + p \rightarrow n + \nu_\mu, \tag{3}$$

has resisted detailed investigation for a number of reasons:

(i) The final state is difficult to detect and, being only a two-body state, it does not have as many measurable parameters as do the three-body states of the first two processes.

(ii) Muon capture in hydrogen is difficult to study experimentally, since only about one μ^- per thousand is captured; furthermore, molecular effects make the comparison with theory difficult.

(iii) Muon capture in the heavier elements is in general difficult to analyze because of the nuclear physics involved.

Radiative muon capture,

$$\mu^- + p \rightarrow n + \nu_\mu + \gamma, \tag{4}$$

is also a difficult process to study experimentally, its rate being about 3000 times smaller than that for ordinary muon capture. In spite of this low rate, however, the process can be profitably studied, since it has the advantages of a three-body final state, one member of which, the γ ray, is readily observable.

Unfortunately, the low rate forces the experimentalist to study the process in elements with $Z \gg 1$; as with normal muon capture, the analysis is then seriously complicated by nuclear effects. In order to minimize the uncertainty of the nuclear effects in the investigation of process (4) reported here, we have chosen Ca⁴⁰ (doubly magic nucleus, $Z = N = 20$) as the capturing medium.

The most easily studied characteristic of the process is the γ-ray spectrum. Although the shape of the spectrum is rather insensitive to the choice of coupling constants, its magnitude is quite sensitive to the value of g_P, the induced pseudoscalar coupling constant. Experimentally, one can easily study only that part of the γ-ray spectrum lying above 50 or 60 MeV; at lower energies, there is considerable contamination from the bremsstrahlung of μ-decay electrons and from nuclear de-excitation γ rays and neutrons following normal muon capture.

Radiative muon capture was first observed by Conforto et al.[1] at CERN; they stopped negative muons in an iron-plate spark chamber, and observed in a thin-plate spark chamber the electron pair produced by the γ ray in a tungsten converter. On the basis of ten events with γ-ray energy above 60 MeV, they obtained a value of the order of 10^{-4} for R, the ratio of radiative to ordinary muon capture. More recently, Chu et al.[2] obtained about 100 events in copper using essentially the same method as the CERN group. Their results give $R = (3 \pm 1) \times 10^{-4}$. The present experiment obtained about 430 γ rays between 60 and 90 MeV, which gave a value for R in agreement with that of Chu et al.

Radiative muon capture is presumably similar in

---

[1] G. Conforto, M. Conversi, and L. di Lella, Phys. Rev. Letters 9, 22 (1962).

[2] W. T. Chu, I. Nadelhaft, and J. Ashkin, Bull. Am. Phys. Soc. 8, 34 (1963); W. T. Chu, Carnegie Institute of Technology Report NYO-10562, 1963 (unpublished).

form to the radiative K capture of an atomic electron. This latter process has been widely investigated both theoretically[3,4] and experimentally.[5,6] The photon spectrum in allowed electron K capture was first derived by Morrison and Schiff several years ago.[3] In their calculation, relativistic effects and the influence of atomic screening were neglected. With $x=k/k_{max}$, the energy of the photon in terms of its maximum energy, the spectrum is given by the simple formula

$$f(x)=(1-x)^2 x, \tag{5}$$

and the value

$$R=\alpha/12\pi=1.94\times 10^{-4} \tag{6}$$

is obtained for the branching ratio of radiative to ordinary K capture. The deviations from Eq. (5) observed at low energies in some of the experiments[6] are fully explained by refinements of the theory.[4] The conclusion of this experimental and theoretical work is that the phenomenon is well understood in terms of a four-fermion coupling with photon emission superimposed in a natural way.

Considerable theoretical work has also been done on radiative muon capture.[7–17] Spectral shapes for capture from light nuclei were first computed by Cantwell.[7] Bernstein,[9] and more recently Lobov,[15] have considered in greater detail radiative muon capture in complex nuclei for a discrete transition to a bound state of the product nucleus. Radiative capture in a complex nucleus has also been treated by Primakoff[11] who used the closure approximation.

The interest of an experimental investigation of the radiative capture of polarized muons by spinless nuclei with $Z\ll 137$ was pointed out by Huang, Yang, and

Lee.[8] These authors showed that as a consequence of parity nonconservation, the γ rays should be emitted with an angular distribution

$$\varphi(\Theta)=1+\alpha P \cos\Theta, \tag{7}$$

where P is the muon polarization and Θ the angle formed by the γ-ray momentum and the muon spin.[18] Under the assumption that only the muon current contributes to the γ-ray emission, the asymmetry parameter α was found to be $+1$ for pure S, T, and -1 for pure A, V, couplings. Bernstein[9] has shown that the effects of parity nonconservation are somewhat reduced by the terms induced by the strong interactions.

The case in which the γ ray is radiated by the nucleon was first considered by Manacher and Wolfenstein.[12] An extensive theoretical investigation of radiative capture of a muon by a free proton can be found in Manacher's thesis,[13] where all of the important diagrams are considered. This "complete" treatment of the problem has been extended recently to the case of doubly closed-shell nuclei by Rood and Tolhoek.[16] These authors use the closure approximation with harmonic oscillator wave functions for the nuclei. They express the rate for radiative capture in terms of that for ordinary capture, since errors in the theory arising from the lack of knowledge of the nuclear structure presumably tend to cancel in the ratio. Their results do, indeed, appear to be rather independent of the nuclear
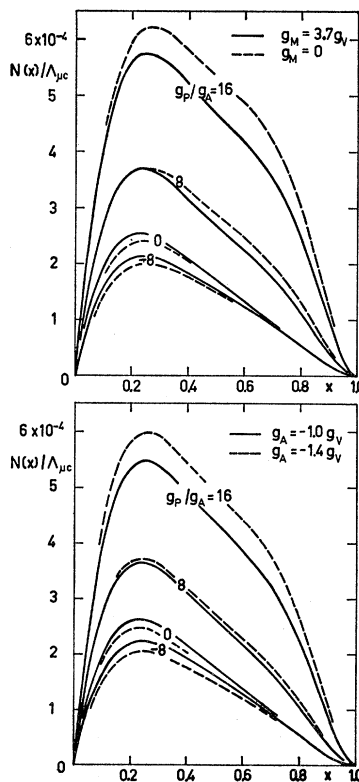
[3] P. Morrison and L. I. Schiff, Phys. Rev. **58**, 24 (1940).

[4] R. J. Glauber and P. C. Martin, Phys. Rev. **104**, 158 (1956); P. C. Martin and R. J. Glauber, *ibid.* **109**, 1307 (1958).

[5] H. Brandt, P. C. Gugelot, O. Huber, H. Medicus, P. Preiswerk, P. Scherrer, and R. Steffen, Helv. Phys. Acta **19**, 222 (1946); D. Maeder and P. Preiswerk, Phys. Rev. **84**, 595 (1951); P. R. Bell, J. M. Jauch, and J. M. Cassidy, Science **115**, 12 (1952); L. Madansky and F. Rasetti, Phys. Rev. **94**, 407 (1954); T. Lindqvist and C. S. Wu, *ibid.* **100**, 145 (1955).

[6] R. J. Glauber, P. C. Martin, T. Lindqvist, and C. S. Wu, Phys. Rev. **101**, 905 (1956).

[7] R. M. Cantwell, Ph.D. thesis, Washington University, 1956 (unpublished).

[8] K. Huang, C. N. Yang, and T. D. Lee, Phys. Rev. **108**, 1340 (1957).

[9] J. Bernstein, Phys. Rev. **115**, 694 (1959).

[10] Y. B. Dai, D. C. San, T. H. Ho, and H. Y. Tzu, Acta Physica Sinica **15**, 262 (1959).

[11] H. Primakoff, Rev. Mod. Phys. **31**, 802 (1959).

[12] G. K. Manacher and L. Wolfenstein, Phys. Rev. **115**, 782 (1959).

[13] G. K. Manacher, Carnegie Institute of Technology Report NYO 9284, 1961 (unpublished); see also G. I. Opat, University of Pennsylvania Report, 1964 (unpublished).

[14] L. N. Chang and Y. B. Dai, Scientia Sinica **10**, 420 (1961).

[15] G. A. Lobov, Nucl. Phys. **43**, 430 (1963).

[16] H. P. C. Rood and H. A. Tolhoek, Phys. Letters **6**, 121 (1963), and to be published; also private communication. See also Ref. 49.

[17] G. A. Lobov and J. S. Shapiro, Zh. Eksperim. i Teor. Fiz. **43**, 1821 (1962) [English transl.: Soviet Phys.—JETP **16**, 1286 (1963)].

[18] See also R. Cutkosky, Phys. Rev. **107**, 330 (1957).

FIG. 1. Theoretical γ-ray spectra of Rood and Tolhoek (Ref. 16) for various values of the coupling constants (assuming the pseudoscalar terms to arise only from one-pion exchange); k_{max} was taken to be 88 MeV. The number of γ rays per muon captured with energy $x=k/k_{max}$ in the interval dx is $N(x)dx/\Lambda_{\mu c}$.

model used: a rough calculation using the statistical model gave results agreeing to within 15% with those of the more precise harmonic oscillator calculations.

Using the formulas of Rood and Tolhoek, we have computed the spectra shown in Fig. 1 for various values of the coupling constants. The figures show a large dependence on the value of g_P, but only a small dependence on g_A and g_M, the axial vector and weak magnetism coupling constants. A measurement of the spectrum can thus be interpreted as a measurement of g_P.

The origin of the induced pseudoscalar term for ordinary muon capture is shown in Fig. 2(a): a virtual charged pion emitted from the "strong" nucleon vertex decays into $\mu + \nu$. To obtain induced pseudoscalar terms for radiative muon capture, one attaches a γ ray to the various lines. Diagrams with the γ ray attached to the nucleon, for example, the diagram of Fig. 2(b), are especially important, since the emission of a large-energy γ ray from the nucleon results in a small denominator for the pion propagator.

The strength of the induced pseudoscalar coupling constant g_P has been widely studied theoretically. Using the empirical value of the renormalized pion-nucleon coupling constant G and the charged pion lifetime, a value of about $\pm 8g_A$ was predicted for g_P by Wolfenstein.[19] Assuming that the charged pion decay proceeds via a nucleon-antinucleon loop, Goldberger and Treiman[20] used a dispersion relation method to resolve the ambiguity in sign; they obtained

$$\frac{g_P}{g_A} \approx \frac{G^2}{8\pi^2} \frac{Mm_\mu}{m_\mu^2 + m_\pi^2} \approx +8, \qquad (8)$$

where m_μ, m_π, and M represent the muon, charged pion, and nucleon masses. The hypothesis of almost conserved axial vector current[21,22] leads to essentially the same result.[23] A number of experiments on ordinary muon capture have been interpreted to give information on g_P,[24–29] the results of which are compared with the results of this experiment in Sec. VI.

FIG. 2. Feynman diagrams showing examples of induced pseudoscalar terms for (a) ordinary muon capture, and (b) radiative muon capture.

Preliminary accounts of the present investigation have been given elsewhere.[30]

II. DESCRIPTION OF THE EXPERIMENT

The experiment was performed at the muon channel of the 600-MeV CERN synchrocyclotron. The machine was operated in the stochastic extraction mode,[31] which gave a duty cycle of $\sim 50\%$ in comparison with the value of $\sim 2\%$ which characterizes the normal operation of such accelerators. This great increase in the duty cycle reduced the accidental coincidence rate to a level which made the experiment feasible, although large corrections still had to be made for accidental events.

The data were obtained in two separate runs, the experimental conditions of which differed only slightly from one another. The setup used in the second run is shown in Fig. 3. In the first run, a plane scintillation counter, with a surface of 35×25 cm², was used instead of the cup-shaped counter D; about 30% of the data were obtained in this manner.

A. Beam and Target

The muon beam was obtained from the decay in flight of negative pions of about 250 MeV/c. The pions were injected by the fringing field of the cyclotron into the muon channel, a system of 24 closely spaced quadrupole lenses.[32] The muons were trapped in the channel with a very high efficiency, almost independent of their emission angle. A strong-focusing bending

[19] L. Wolfenstein, Nuovo Cimento 8, 882 (1958).
[20] M. L. Goldberger and S. B. Treiman, Phys. Rev. 111, 354 (1958).
[21] Y. Nambu, Phys. Rev. Letters 4, 380 (1960).
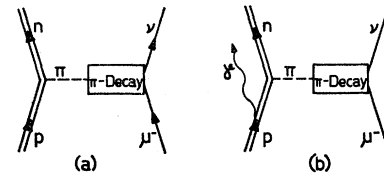[22] J. Bernstein, S. Fubini, M. Gell-Mann, and W. Thirring, Nuovo Cimento 17, 757 (1960).
[23] A. Fujii, Nuovo Cimento 27, 1025 (1963).
[24] J. E. Rothberg, E. W. Anderson, E. J. Bleser, L. M. Lederman, S. L. Meyer, J. L. Rosen, and I. T. Wang, Phys. Rev. 132, 2664 (1963); see also for references to other experiments on muon capture in hydrogen.
[25] I. V. Falomkin, A. I. Filippov, M. M. Kulyukin, B. Pontecorvo, Yu. A. Shcherbakov, R. M. Sulyaev, V. M. Tsupko-Sitnikov, and O. A. Zaimidoroga, Phys. Letters 3, 229 (1963); L. B. Auerbach, R. J. Esterling, R. E. Hill, D. A. Jenkins, J. T. Lach, and N. H. Lipman, Phys. Rev. Letters 11, 23 (1963), and Proc. Sienna Intern. Conf. on Elementary Particles 1, 61 (1963); R. M. Edelstein, D. Clay, J. W. Keuffel, and R. L. Wagner, Jr., in Proceedings of the Brookhaven International Conference on Weak Interactions, 1963, p. 303 (unpublished).
[26] R. C. Cohen, S. Devons, and A. D. Kanaris, Phys. Rev.

Letters 11, 134 (1963), and Nucl. Phys. (to be published). We thank these authors for sending us their unpublished results. A. Astbury, L. B. Auerbach, D. Cutts, R. J. Esterling, D. A. Jenkins, N. H. Lipman, and R. E. Shafer, Nuovo Cimento 33, 1020 (1964).
[27] T. Ericson, J. C. Sens, and H. P. C. Rood, Nuovo Cimento (to be published).
[28] V. S. Evseev, V. S. Roganov, V. A. Chernogorova, M. M. Szymczak, and Chang Run-Hwa, Phys. Letters 6, 332 (1963); see also for references to other neutron asymmetry experiments.
[29] E. J. Maier, R. M. Edelstein, and R. T. Siegel, Phys. Rev. 133, B663 (1964); see also for references to other experiments of muon capture in C¹².
[30] M. Conversi, R. Diebold, and L. di Lella, Congressino Annuale dell'Istituto Nazionale di Fisica Nucleare, Frascati, May 1963, LNF-63/47, p. 124 (unpublished); International Conference on Fundamental Aspects of Weak Interactions, 1963 [Brookhaven National Laboratory Report BNL-837, 1963 (unpublished), p. 314]; Proc. Sienna Intern. Conf. on Elementary Particles 1, 53 (1963).
[31] L. Dick and J. Vermeulen (to be published).
[32] A. Citron, C. Delorme, F. J. M. Farley, L. Goldzahl, J. Heintze, E. G. Michaelis, M. Morpurgo, and H. Øverås, Proceeding of an International Conference on Instrumentation for High-Energy Physics, Berkeley, 1960 (Interscience Publishers, Inc., New York, 1961), p. 286; A. Citron, M. Morpurgo, and H. Øverås, CERN report 63-35, 1963 (unpublished).
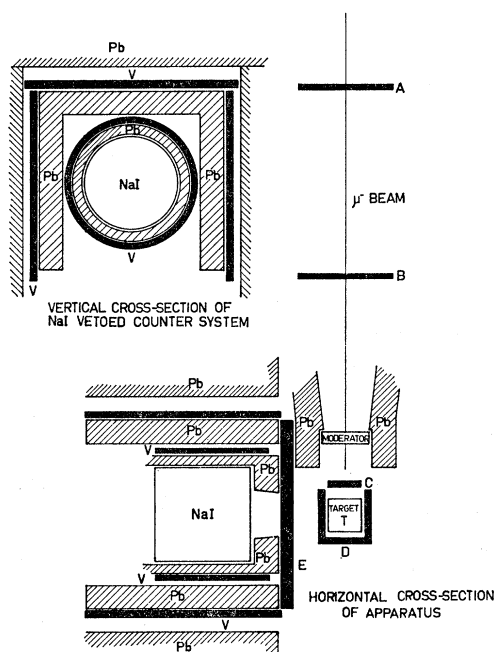
FIG. 3. Sketch of the experimental setup used in the second half of the experiment (very similar to that of the first half).

magnet at the end of the channel selected the muons emitted backward in the pion c.m. system. The nearly pure 80-MeV kinetic energy muon beam obtained in this way was then transported to the calcium target by four quadrupole lenses. These lenses were also useful in shielding the experiment from the reaction products of those pions which had not decayed, and which were stopped in the yoke of the bending magnet. The particle flux through counters A and B (see Fig. 3) was $\sim 70\,000$/sec.

After crossing the moderating copper plate (2.4 cm thick) and counter C, the muons came to rest in the target T, a Ca^{40} cube 7 cm on each side. A muon stop in T was defined electronically as $ABC\bar{D}$; the average rate of these events was about 5000/sec.

It is almost needless to stress the advantage of a method by which also the low-energy part of the γ-ray spectrum from radiative muon capture can be explored. Apart from the increased rate of recorded events, the experimental value of the branching ratio R would no longer depend on the unknown nuclear structure effects, at least in the ideal case in which γ rays of all possible energies were detected. In preliminary runs, attempts were made, therefore, to develop a method suitable to reject with high efficiency the overwhelming background due to bremsstrahlung of decay electrons from μ^- mesons which escaped nuclear capture, and thereby to record also fairly low-energy γ rays from process (4). For this purpose, a liquid scintillator loaded with silicon was used as a sensitive target. The pulses produced in such a target by the decay electrons were used to anticoincide the bremsstrahlung background associated with the

electrons themselves. These attempts failed, however, partly because of a comparatively large contribution of high-energy neutrons and γ rays from nuclear de-excitation following ordinary muon capture, and partly because of an apparently unavoidable vetoing of "good" events, which will not be discussed here.

B. Detection of the γ Rays

The γ rays from radiative muon capture in the target were detected by a cylindrical NaI crystal with a diameter and a height of 20 cm. Its scintillation light was collected by three 5-cm photomultipliers (Philips 56 AVP). In order to obtain the best possible energy resolution, the voltages of the three photomultipliers were adjusted to give equal outputs when a Cs^{137} radioactive source was placed at the centre of the crystal face. The stability of the counter was improved by keeping constant the temperature of the crystal, and by using low-drift resistances in the voltage divider chains of the photomultiplier bases.

A 5-cm-thick lead collimator, coaxial with the crystal, was placed in front of the counter. This collimator defined the solid angle and improved the energy resolution by accepting only those γ rays entering the crystal close to its axis. The collimator was conically shaped, its diameter varying from 10 cm at the front face to 9 cm at the rear face (target side, see Fig. 3).

Particular care was taken to minimize the effects of the background counting rate of the NaI counter. Events of random nature were produced by particles which, although uncorrelated with a muon stopping in T, gave a pulse in the NaI counter soon enough after the muon stop (and large enough) to simulate a radiative capture event.

The number of such events was, of course, proportional to the effective background counting rate of the NaI counter, and great care was taken to reduce this rate. The counter was surrounded by a double layer of thick lead shielding with a system of vetoing counters V; this reduced the cosmic ray and machine background considerably. A concrete hut, 80 cm thick, was then built around the apparatus to further reduce background. Prompt events were eliminated by vetoing with counters A and C, and charged particles from the target were vetoed by counter E. The net result of all this shielding and vetoing was that we effectively had only 0.2 counts per second between 60 and 90 MeV.

Because of the long decay constant (250 nsec) of the scintillation light in the NaI crystal, it was impossible to have both good time and good energy information in the same pulse. For this reason, three different outputs from the NaI counter were used:

(1) The anode pulses of the three photomultipliers were summed together and clipped to give a very fast pulse with practically no energy information;

(2) the dynode 14 pulses were treated to give a

moderately fast pulse which was used to decide whether or not the event was energetic enough to warrant recording;

(3) a very slow integrated pulse from the ninth dynodes was fed into a pulse-height analyzer to measure the energy of the γ ray.

The energy resolution of the NaI crystal has been measured using radioactive sources and momentum-analyzed electron beams.[33,34] For γ-ray energies ≈ 1 MeV, the resolution function is symmetric with a full width at half-maximum of about 8%. In the energy range of interest to this experiment, the resolution function is quite asymmetric and has a width of 17% (see Fig. 4, dashed curve). Cocconi et al.[33] found the shape to be independent of energy from 25 to 110 MeV. The average energy loss (by the shower partially escaping from the crystal) represented by the long, low-energy tail is $\sim 9\%$ if one assumes the peak energy to be that of the electron. This energy loss is perhaps slightly less than might have been expected from shower measurements in tin.[35]

The stability of the system was frequently checked with a Na^{22} source (γ rays of 0.51 and 1.28 MeV) during the runs. This method was sensitive to drifts in the light output from the crystal, the phototube responses, and the electronic amplification. The system was found to be quite stable ($\lesssim 1\%$ drift/week).

C. Calibration of the NaI Crystal

The crystal was calibrated with the sharp high-energy cutoff of the electron spectrum from μ decay. Negative muons were stopped in a 5-mm-thick plastic scintillation counter placed at 30° with respect to the beam direction. In the plastic, the muons quickly fell into orbits about the carbon atoms, from which approximately 90% of them decayed, emitting an electron. The pulse-height analyzer was gated by a coincidence between the target counter and a 15-mm-thick plastic scintillation counter placed in front of the crystal; the results are shown by the points in Fig. 4.

The resolution of the crystal was folded into the decay electron spectrum (calculated by Überall[36] for muons bound in carbon), and the resulting curve was least squares fit to the high-energy experimental points by adjusting two parameters: (i) the energy scale factor of the experimental points (taking into account the energy losses in the scintillation counters); and (ii) the normalization. The best fit curve is shown in Fig. 4 (χ^2 is 42 for 35 degrees of freedom).

[33] V. T. Cocconi, T. Fazzini, G. Fidecaro, M. Legros, N. H. Lipman, and A. W. Merrison, Nuovo Cimento 22, 494 (1961).
[34] G. Conforto, M. Conversi, L. di Lella, G. Penso, C. Rubbia, and M. Toller, Nuovo Cimento 26, 261 (1962).
[35] R. Hofstadter, in Methods of Experimental Physics 5A, edited by Luke C. L. Yuan and Chien-Siung Wu (Academic Press Inc., New York, 1961), p. 652.
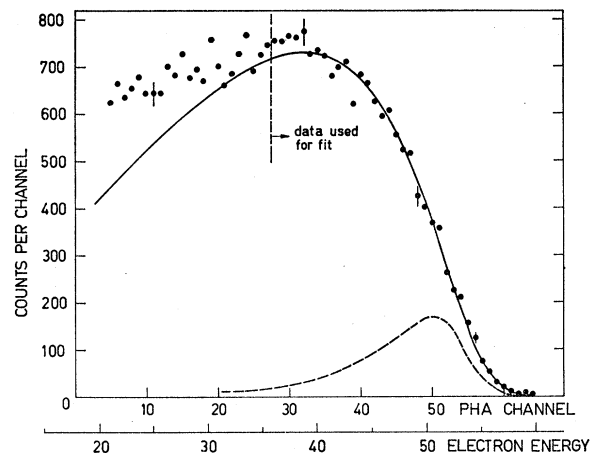[36] H. Überall, Phys. Rev. 119, 365 (1960).

FIG. 4. Spectrum of electrons from the decay of muons (stopped in plastic) as measured by the NaI crystal; typical statistical errors are shown. The solid curve is the spectrum calculated by Überall (Ref. 36) and spread by the NaI crystal resolution (shown by the dashed curve). The theoretical spectrum was least squares fit to the experimental points above ~ 35 MeV to give the calibration of the NaI crystal; this calibration was used to obtain the electron energy scale (corrected for energy losses in the scintillation counters).

The low-energy background apparent in the figure does not appreciably affect the determination of the energy scale factor (the bset value for this number was found to be insensitive to the inclusion or omission of the low-energy points in the fit.)

The result of the calibration indicated that the response of the system was $\sim 10\%$ lower than one would have expected on the basis of the radioactive source measurements. Such a result is perhaps not surprising when compared with the results of Iredale,[37] who found that for γ rays the light output of NaI crystals divided by the γ-ray energy dropped by 20% in going from 0.05 to 1.33 MeV.

The quality of the fit of the curve to the experimental points in the region of the sharp cutoff is quite sensitive to the width assumed for the NaI counter resolution. The reasonably good fit to the data allows us to conclude that the effective width of the resolution is not significantly different from that which had been assumed.

D. The Electronics

A simplified block diagram of the electronics employed in the experiment is shown in Fig. 5. We shall discuss the logical functions of the equipment without going into the details of the working principles of the circuits, which were mostly of standard type.

The problem of random events discussed previously could not be solved by fast circuits, since the good events are distributed exponentially in time following the muon stop; the time constant, of course, is just the muon lifetime in calcium, 345 nsec. Because of this

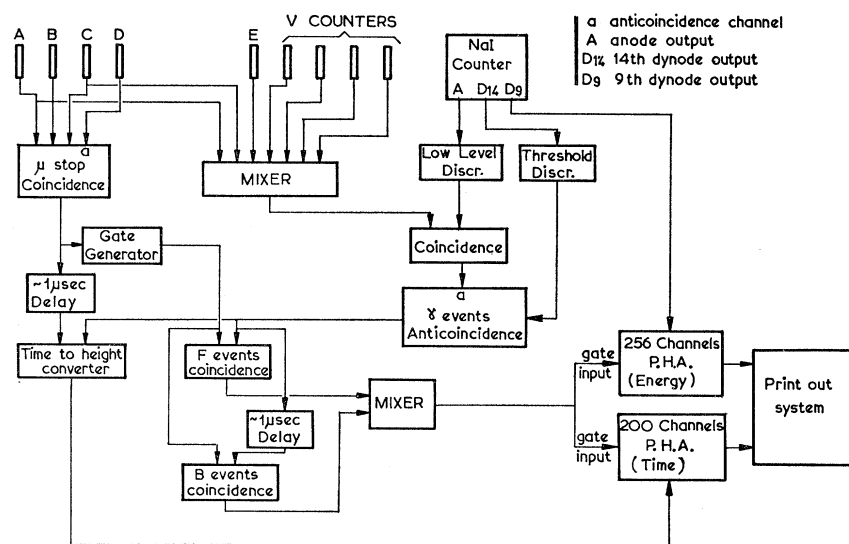[37] P. Iredale, Nucl. Instr. Methods 11, 336 (1961).

FIG. 5. Simplified block diagram of the electronics.

distribution in time, we accepted NaI pulses within a time interval of 612 nsec which was defined by a gating circuit opened by the muon stop signal, $ABCD$. Because of this wide acceptance in time, "foreground" or F events, i.e., the events falling in this gate, were highly contaminated by random coincidences between an uncorrelated NaI pulse and the 612-nsec gate pulse. Accidental background events (B events) were recorded continuously during the runs by looking at the NaI counter pulses which were in a second time interval, the "B" gate. The length of the "B" gate was essentially the same as that of the "F" gate, but by means of electronic delays it was made to precede in time the muon stops. Thus, the difference $F-B$ for events lying in the same energy interval gave the number of causal events in that particular energy interval.

The detection threshold for the γ events was set at about 45 MeV by discriminating against smaller pulses from the 14th dynodes. Because of the long decay constant of scintillation light in NaI, the output signal of the discriminator was affected by a jitter of about 50 nsec (caused by the statistical fluctuation in the number of photoelectrons in the photomultipliers). The pulse obtained from the discriminator was therefore not suitable for use with the veto counters A, C, E, and V. A jitter-free pulse from the NaI counter was obtained by feeding the anode output to another discriminator, whose bias was set at a very low level (corresponding to ~ 0.2 MeV). The output signal from this circuit was affected by a jitter of less than 5 nsec for events exceeding the γ event threshold. The signal from the anode discriminator was clipped to a length of ~ 15 nsec and put in coincidence (~ 30-nsec resolving time) with a signal obtained by mixing together the pulses from counters A, C, E, and V. Whenever such a coincidence took place, a 400-nsec pulse was generated

which vetoed with the output signal from the threshold discriminator. The γ events which survived this veto circuit were fed (both directly for F events, and through a 1-μsec delay for B events) to the gate circuits opened by muon stops.

The time interval (positive or negative) between the muon stop and the NaI pulse was measured by means of a time-to-height converter[38] which used as time base the sweep generator of a Tektronix 585 scope, set for a 2 μsec sweep. The circuit was started by the NaI pulse, and stopped by the muon stop pulse delayed artificially by about 1 μsec. NaI pulses simultaneous with muon stops fell in the center of the linearity interval, allowing one to explore a time interval going from ~ -1 to $\sim +1$ μsec with respect to a muon stop. The output of the time-to-height converter was sent to a 200-channel pulse-height analyzer (time PHA). The position of the "zero time" channel was measured by sending π^- mesons through the target; counters A, C, and E were disconnected from the veto logic, allowing the NaI counter to detect secondaries from π^- stars in the target. This process is very fast, of course, and the time distribution showed a very sharp peak.

The slow integrated pulse from the 9th dynodes of the NaI photomultipliers was fed to a 256-channel pulse-height analyzer (energy PHA), through a highly stable linear amplifier. The gain of this amplifier was increased by a factor ~ 60 for the radioactive source calibrations.

During the main runs, the energy and time PHA gates were opened only if an F or B event took place. The energy and time of each event was recorded by a trick involving the mode of operation of the PHA's: to measure the amplitude of a pulse, the PHA's convert the amplitude into a time interval and count the number

---

[38] J. Fischer and A. Lundby, Rev. Sci. Instr. **31**, 10 (1960).

of waves from a standard oscillator which fall in that interval. We fed these wave trains from the two PHA's into two 25-Mc/sec scaler units,[39] the contents of which were printed out for each F or B event and then reset. The rest of the electronics was paralyzed during the printing, which took about one second per event.

Such a method of recording the main information about each event allows one to order the events in matrix form: N_{ik}, the general element of this matrix, being the number of events located simultaneously in the ith channel of the energy PHA and the kth channel of the time PHA. F and B events thus fall into two completely separated regions of the matrix. After the runs, the printouts from the two scalers were copied onto perforated paper tape and fed into the CERN Mercury computer which constructed the matrix N_{ik}.

III. DATA REDUCTION

Let $N(x)$, with $x = k/k_{max}$, represent the unknown differential energy spectrum of γ rays from process (4), normalized so that

$$(1/\Lambda_{\mu c}) \int_0^1 N(x) dx = R,$$

where $\Lambda_{\mu c}$ is the rate for μ^- capture in Ca⁴⁰. The experimental spectrum $N(x)/\Lambda_{\mu c}$ was obtained from the relation

$$C_i = N_\mu - \epsilon u f \frac{\omega}{4\pi} \frac{N(x)\Delta x_i}{\Lambda_{\mu c}}. \qquad (9)$$

We now define and discuss the various factors of this equation and their uncertainties.

A. The Corrected Number of γ Rays C_i Observed in the Energy Range Δx_i

The number of "F" events observed in the gate following the muon stops had to be corrected for a number of effects. The largest correction was for random events; this correction was made by subtracting the events in the negative time gate (corrected for a 2.4% difference in gate widths) from those in the positive time gate. Between 60 and 90 MeV, there were nearly as many random events as causal events, giving an average increase in statistical error of ~ 1.7 over the ideal case of no random events.

For the low-energy ($E \lesssim 60$ MeV) events, corrections had to be made for the contributions from bremsstrahlung from μ-decay electrons, and for contributions from those μ-decay electrons ($\lesssim 4\%$) which escaped vetoing by counter E. Estimates of these contaminations were obtained by approximate, analytic methods which averaged over the μ-decay electron spectrum and the decay position in the calcium target. The electron spectrum was

---

[39] F. Iselin, Nucl. Instr. Methods 20, 330 (1963).

obtained from the formula of Überall.[36] The resolution of the NaI crystal was folded into the results of the calculations to give the number of contamination events expected per pulse-height analyzer channel. It was found that after subtracting this number from the counting rate, there was still an excess of events below 60 MeV; this excess of low-energy is discussed in Sec. IV. Because of the uncertainty of the contamination at low energies, we consider only the data above 60 MeV to be reliable, and have used only these data for the analysis.

The experimental counting rate also had to be corrected for those high-energy γ rays which materialized in the edge of the lead collimator, but were still able to produce a large pulse in the NaI crystal. This correction was 2.4% at 60 MeV, and was less at higher energies.

Approximately 20% of the muons stopped in counter C; due to the long μ^- lifetime in the plastic scintillator, these muons had a much smaller probability of being captured in the gate interval than did those stopping in the calcium target. Their contribution of radiative capture γ rays was only 1% of the total, assuming the ratio of radiative to ordinary muon capture to be the same for carbon and calcium.

A $(1.0 \pm 0.5)\%$ correction was applied to the data to take into account vetoing of γ rays by some of the shower escaping from the NaI crystal and striking one of the counters V. This effect was measured by passing an electron beam into the crystal and observing the counting rate with and without the V counters in anticoincidence.

B. The Effective Number of Muon Stops, N_μ

The electronic definition of a muon stop, $ABC\bar{D}$, had to be corrected for several effects. The largest correction ($\sim 20\%$) was for muons which stopped in counter C or in the thin dead layer of counter D. The number of muons stopping in these counters and giving a μ-stop signature was experimentally determined by observing the muon stopping rate (normalized to the monitor rate AB) with and without the calcium target. A run without calcium, but with a sheet of plastic immediately behind counter C, indicated that the coincidences $ABC\bar{D}$ without calcium were mainly muons stopping in counter C.

After stopping in the target, the muons quickly become atomically bound to the calcium; in the process, characteristic mesic x rays are emitted. Approximately 1.5% of the times, one of the more energetic of these x rays entered the NaI crystal, giving a pulse in coincidence with the beam counters. This produced a long (400 nsec) veto pulse, and a 1% correction was applied to take this vetoing effect into account.

Corrections were also made for beam contamination. The pion contamination was $\sim 0.15\%$, and the electron

contamination $(2\pm1)\%$.[40] Only about one-third of the electrons can simulate a muon stop, however, giving a total beam contamination correction of $(0.8\pm0.5)\%$.

A further correction of 0.3% was applied to take into account dead-time effects associated with the μ-stop gate.

Applying all these corrections to the electronic definition $ABC\bar{D}$, we obtained 0.52×10^9 effective muon stops for the first run, and 1.11×10^9 for the second run. The total number of effective muon stops was thus

$$N_\mu = 1.63\times10^9.$$

C. The Fractional Solid Angle $\omega/4\pi$

The solid angle for γ rays entering the NaI crystal was limited by the 5-cm-thick lead collimator; the edge of the collimator was not well defined, since the γ-ray mean free path in lead is about 1 cm. Thus the γ rays traveling through one or two centimeters of the rear corner of the opening had a reasonable chance of not materializing, or of materializing sufficiently close to the rear edge of the wall that the shower did not lose much of its energy in the lead. For practical reasons, we were unable to veto such showers by placing counter E behind the wall; instead, we made corrections to the counting rate as discussed previously. Since C_i is the number of nonconverting γ rays, the value of ω needed for Eq. (9) is the average solid angle for a γ ray to reach the crystal without converting in the collimator. This means that instead of being defined by the opening at the rear of the collimator, the solid angle was effectively defined by the edge of the opening, one γ-ray mean free path from its rear edge. The solid angle subtended by this effective circular opening was averaged over the target volume, taking into account the muon stop distribution which was measured in a special run (and found to be nearly uniform). The results of this calculation gave

$$\omega/4\pi = 0.0166.$$

D. Probability ε for γ Rays to Escape Vetoing by Counter E

To avoid being vetoed by counter E, the γ rays had to pass through the calcium target, counter D, and most of E, without materializing. The probability for not materializing was calculated using the mean free paths for 68-MeV γ rays in calcium and plastic (18.7 and 73 cm, respectively). An average was made over the target volume, but no correction ($\lesssim1\%$) was made for those showers which were not vetoed because they consisted entirely of photons when passing through counter E. The results for the two sets of runs were

$$\epsilon_1 = 0.813, \quad \epsilon_2 = 0.800.$$

E. Fraction u of Muons Disappearing in the Gate Interval

The fraction of muons which disappear (i.e., decay or are captured) during the μ-stop gate is

$$u = e^{-t_1/\tau^-}(1 - e^{-\Delta t/\tau^-}),$$

where $\tau^- = (345\pm3)$ nsec[41] is the μ^- lifetime in Ca^{40}, t_1 is the length of time between the muon stop and the opening of the gate (85 and 50 nsec for the first and second set of runs, respectively), and Δt is the gate length $= 612$ nsec (~1.8 lifetimes). The formula gives

$$u_1 = 0.650, \quad \text{and} \quad u_2 = 0.717.$$

F. Fraction f of μ^- in Ca^{40} which Are Captured

The fraction of muons which are captured (instead of decaying) is

$$f = \Lambda_{\mu c}/\Lambda^-_{total} = 1 - \Lambda^-_{decay}/\Lambda^-_{total},$$

where Λ^- refers to the rates of the various processes for negative muons in Ca^{40}. The μ^- decay rate is approximately (to within one or two percent) just the μ^+ decay rate, i.e.,

$$\Lambda^-_{decay} \approx \Lambda^+_{decay} = 1/\tau^+.$$

Using this relation, we find

$$f = 1 - \tau^-/\tau^+ = 0.843.$$

G. Errors

A small error arises from the fact that we have neglected the polarization of the muons. The beam was about 85% polarized in a sense opposite to its laboratory momentum.[32] The counting rate of γ rays from radiative capture is

$$C = C_0(1 + \alpha P \cos\Theta),$$

where C_0 is the rate for unpolarized muons which we wish to compare with theory; α is the asymmetry coefficient, predicted to be[9] ~0.8; P is the residual muon polarization after atomic capture; and Θ is the angle between the direction of polarization and the γ-ray momentum. Since the magnetic field at the target position was 3.6 G, the muons precessed by about 0.1 rad in one lifetime. If we assume the same residual muon polarization as that of Ref. 28, the ratio C/C_0 in our experiment would differ from unity by about $0.8\times0.19\times0.1 = 1.5\%$. But the residual polarization of the muons was not measured in our experiment; thus no attempt was made to correct for this small effect.

By far the largest systematic uncertainty (apart from the question of possible unknown contamination) is that of the NaI resolution. The resolution function discussed previously was obtained with electrons entering the crystal along its axis. The skewness of this curve

[40] A. Citron, C. Delorme, D. Fries, J. Heintze, E. G. Michaelis, H. Øverås, and Yu. A. Shcherbakov, Nucl. Instr. Methods **15**, 121 (1962); A. Citron (private communication).

[41] W. A. Cramer, V. L. Telegdi, R. Winston, and R. A. Lundy, Nuovo Cimento **24**, 546 (1962).

represents an average escape of shower energy from the crystal and results in our obtaining fewer high-energy pulses than if the resolution were symmetric. In our experiment the γ rays can enter the crystal off axis and at large angles with respect to the axis. Under such conditions the resolution function may become even more asymmetric, i.e., a greater fraction of some of the showers may escape from the crystal. An indication that the effect is not serious can be obtained from the results of Cocconi et al.[33] They found no difference in resolution when their positron beam size was increased from 5 to 9.5 cm in diameter. Their situation was somewhat better than ours in that their beam was parallel to the crystal axis, although this probably did not make a great deal of difference, since multiple scattering and shower development in the crystal tend to destroy the effects of beam collimation. There is a second effect which could make our resolution more skewed than theirs: we measure γ rays (instead of positrons) which have a conversion length in NaI of $\sim$4 cm, and in unfavorable cases can migrate close to the edge of the crystal before materializing.

No correction has been made for these effects. We feel that at most they lead to an error in $N(x)/\Lambda_{\mu c}$ of a few percent, and we have included a systematic error of 10% in the calculations of the final results for g_P.

IV. DATA ANALYSIS

The corrected experimental values for the differential energy spectrum of γ rays from process (4), $N(x)/\Lambda_{\mu c}$, are shown as the circular points in Fig. 6, and are listed in Table I. These values were obtained from Eq. (9) as described in the previous section, and represent an average of the two separate epxerimental runs (Sec. II). Note that a definite value for $k_{\max}$ must be assumed, since equation (9) has a factor $1/\Delta x = k_{\max}/\Delta k$; the value $k_{\max} = 88$ MeV was assumed. The triangular points in the low-energy region are values of $N(x)/\Lambda_{\mu c}$ not corrected for contamination from muon decay electrons and their bremsstrahlung. The difference between the triangular and circular points thus gives an indication of the importance of this correction. It is seen that, although important at low energies, the contamination is expected to be negligible above 58 MeV. At high energies, the errors shown are statistical only; at low energies, they also include the uncertainty of the contamination corrections.

As an internal consistency check, the experiment was divided into three roughly equal parts: run I, run IIa and run IIb. Runs IIa and IIb were taken (in June 1963) with the same experimental setup, one after the other; in run I, carried out two months earlier (April 1963), the experimental setup was slightly different, as mentioned in Sec. II. For each run, Eq. (9) was used to compute the integral

$$I(k_{\min} = 60.6 \text{ MeV}) = \int_{k=60.6 \text{ MeV}}^{k=100 \text{ MeV}} \frac{N(x)}{\Lambda_{\mu c}} dx, \quad (10)$$
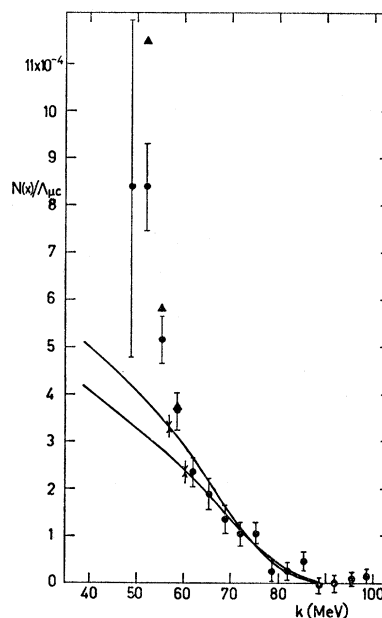

FIG. 6. The experimental γ-ray spectrum. The circular points are values corrected for the calculated contamination from muon-decay electrons and their bremsstrahlung. In the low-energy region where the correction was necessary, the uncorrected points are shown as triangles. The error flags on the points represent the statistical and contamination calculation uncertainties. For the numerical calculation of the points, it was assumed that $k_{\max} = 88$ MeV. The curves are best fits (see text for details) to the data above 57.0 (top curve) and 60.4 MeV (lower curve).

i.e., for each run the number of events between 60.6 and 100 MeV was normalized to the same number of muon stops, etc. The results (see Table II) have a large spread, giving $\chi^2 = 6.4$ for two degrees of freedom ($P_{\chi^2} = 4\%$). Even runs IIa and IIb do not agree well with each other ($\chi^2 = 4.2$ for one degree of freedom, for which $P_{\chi^2} = 4\%$). A large part of this apparent inconsistency stems from an abnormally low counting rate in

TABLE I. The experimental spectrum corrected for contamination. The errors represent both the statistical and contamination uncertainties. In calculating the numerical values, it was assumed that $k_{\max} = 88$ MeV.

k	x	$N(x)/\Lambda_{\mu c} \times 10^4$
48.7 MeV	0.554	8.38±3.56
52.0	0.591	8.39±0.92
55.4	0.630	5.16±0.49
58.7	0.667	3.64±0.39
62.1	0.705	2.35±0.32
65.4	0.743	1.89±0.32
68.7	0.780	1.34±0.29
72.1	0.819	1.03±0.26
75.4	0.856	1.05±0.24
78.8	0.895	0.26±0.22
82.1	0.933	0.25±0.20
85.4	0.970	0.46±0.19
88.8	1.009	−0.04±0.18
92.1	1.047	−0.01±0.18
95.5	1.085	0.08±0.16
98.8	1.122	0.14±0.15

TABLE II. Comparison of the normalized number of counts collected in the interval $60.6 < k < 100$ MeV by the three runs. For $k_{max} = 88$ MeV this normalized counting rate is equivalent to

$$I(x=0.69) = \int_{0.69}^{1.14} \frac{N(x)}{\Lambda_{\mu c}} dx.$$

Run	$I(x=0.69) \times 10^4$
I	0.398 ± 0.060
IIa	0.222 ± 0.050
IIb	0.366 ± 0.049
Average	0.322 ± 0.030

the first half of run IIa. At this time, the box counter D was temporarily in anticoincidence with the NaI crystal. Thus, if radiative muon capture events were detectable in counter D (which together with counter C completely surrounded the target), the counting rate would be lower than normal. Calculations were made of the efficiency for detecting neutrons emitted following μ^- capture, but could account for at most a 5% drop in the counting rate, compared with the drop of $(40 \pm 20)\%$ observed.

Since the measurements were taken with the same setup, and checks were made frequently on the equipment, it is difficult to see any real reason why runs IIa and IIb should give different results. Similarly, there is no reason to suspect that there should be a real difference between runs I and II, since they were made with nearly the same setup and the equipment was intercalibrated. Thus, our feeling is that the spread in the results is probably of a statistical nature.

Two other consistency checks were made of the data. The first was intended to make sure that there was no appreciable background, other than random events, at high energies. It was found that there were 10 ± 30 nonrandom events with energy greater than 100 MeV (compared with 430 between 60 and 100 MeV); it was thus concluded that there was no significant high-energy background.

As a further consistency check, we verified that the events in the energy range of interest (60 to 100 MeV) had the appropriate time distribution after being corrected for random background. A fit to the data was made using an exponential function of the form $A \exp(-t/\tau)$, A and τ being the fitting parameters. The best fit ($\chi^2 = 6.6$ for 8 degrees of freedom) was obtained for $\tau = (339 \pm 26)$ nsec, in good agreement with the accurate determination [(345 ± 3) nsec] of the μ^- lifetime in Ca^{40} by Cramer et al.[41] The time distribution of our events in the energy range of interest is shown in Fig. 7.

The spectra of Rood and Tolhoek[16] for Ca^{40} were used to fit the experimental results to possible values of the coupling constants. Sets of coupling constants were fed into an IBM-7090 computer program, and the corresponding differential energy spectra $N(x)/\Lambda_{\mu c}$ were computed for each set. The NaI crystal energy resolu-

tion was folded into each theoretical spectrum to give the spectrum which would be measured by the crystal if the theory were correct and that particular set of coupling constants were the true, physical set. From this spectrum, distorted by the experimental resolution, the number of counts expected per energy interval was calculated and compared with the experiment. This comparison was made assuming various values of k_{max} for each spectrum, and the "best" value for k_{max} (i.e., the best fit to the experimental data) was obtained by the method of least squares. Changing k_{max} not only shifted the trial spectrum along the energy scale, but it also changed the amplitude by a factor of K^2_{max} to take into account a phase-space factor in the theory; as mentioned previously, there is also a factor of k_{max} in the experimental determination of $N(x)/\Lambda_{\mu c}$. Comparing the fits obtained by spectra with different values of g_P gave the most likely value of g_P, for a given choice of the other coupling constants. Unfortunately, the data were insufficient to allow one to fit more than one coupling constant at a time.

As might be expected, the best values for g_P and k_{max} were strongly correlated; this is shown in Fig. 8, where the curves trace out values of k_{max} and g_P which have equal likelihoods. For example, if g_P is large, the spectrum will have a large magnitude and thus needs to be shifted to the left (i.e., small k_{max}) to give the best fit. This correlation results in larger statistical uncertainties in k_{max} and g_P than would be the case if one or the other were considered as known.

The best fit values of g_P and k_{max} are shown in Fig. 9 as a function of k_{min}, the low-energy cutoff for data used in the fit. (Caution must be exercised in the interpretation of the figure, since the errors are not independent.) The rapid increase in g_P below 60 MeV indicates that the data in this region do not have the spectral shape expected. This can also be seen in Fig. 6, where the best fit spectra for $k_{min} = 57.0$ and 60.4 MeV are compared with the experimental points; below 60 MeV the points, corrected for contamination, are still higher than expected. For example, comparing the value of $N(x)/\Lambda_{\mu c}$ measured directly at 59 MeV with that indicated by the fit to the data above 60.4 MeV, gives
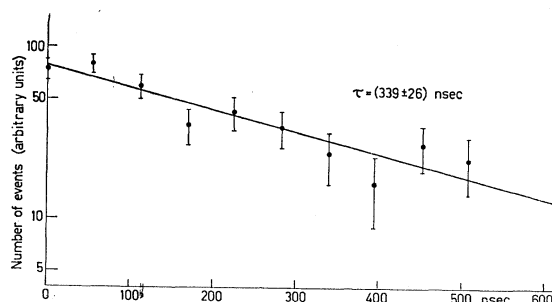

FIG. 7. Experimental time distribution of the events in the energy interval from 60 to 100 MeV, after subtraction of the accidental background.
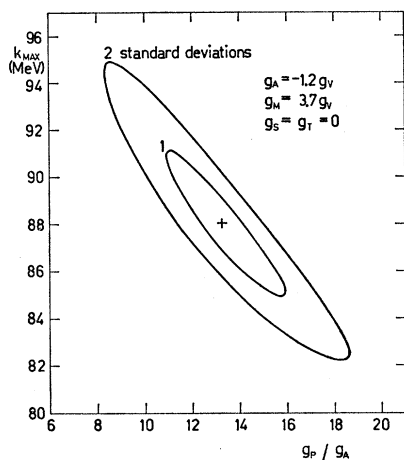
FIG. 8. Lines of equal probability in the g_P, k_{max} plane as given by our experimental data. The contour marked "1 standard deviation" has $X^2 = X_0^2 + 1$, where X_0^2 is the least-squares value; contour 2 has $X^2 = X_0^2 + 4$. Statistically one expects the inner curve to enclose the physical point g_P, k_{max} with a 40% probability, and the outer curve with an 86% probability. It is seen that there is a strong correlation between g_P and k_{max}.

$X^2 = 4$ for 1 degree of freedom $(P_{X^2} = 4\%)$. At lower energies the discrepancy becomes worse.

There are several possible explanations of this low-energy discrepancy though none of them, except possibly the last, seems to be very satisfactory:

(1) The shape of the γ-ray spectrum of radiative muon capture which was theoretically predicted might be different from the real spectrum. This would require a major revision of the theory, however.

(2) The contamination calculation might be inaccurate. If this was the reason for the discrepancy, the calculation must be much worse than estimated, since the discrepancy is considerably larger than even the rather liberal errors given the points in Fig. 6 to take into account the approximate nature of the calculations.

(3) The energy calibration of the NaI counter might be too high by about 6%; i.e., the true γ-ray energies of the experimental points might be really lower than had been thought, and larger contamination corrections should thus be subtracted from the points. It is interesting to note that the energy calibration of the NaI counter thus suggested is about midway between that obtained from radioactive sources and that obtained by looking at the muon decay electron spectrum; there is, however, no other reason to doubt the latter calibration.

(4) The resolution of the NaI counter might be considerably wider than had been thought, allowing more of the contamination to appear in the higher energy channels. This possibility seems to be ruled out by the good fit to the high-energy muon decay electrons which was obtained when calibrating the NaI counter.

(5) Ordinary muon capture might occasionally give a large fraction of the available energy to the capturing nucleus, which then emits a γ ray or neutron (which

could produce in the NaI crystal a star or knock-on proton of 50 or 60 MeV).

In connection with this last possibility, we have tried to make estimates of the high-energy neutron spectral shape from ordinary muon capture. To this end we have used a somewhat crude theory[42] relating this spectrum to that obtained in neutron photoproduction. Unfortunately, data on neutron photoproduction in Ca⁴⁰ do not exist and one must use data from O¹⁶ to obtain an estimate of the spectral shape. We then normalized the spectrum to agree with the number of neutrons found above 20 MeV by Hagge.[43] The number of neutrons above 60 MeV estimated in this fashion is about the same as the number of events found by our experiment in this region. For a neutron to be counted, however, it would have to interact in the NaI crystal in such a manner as to give a large fraction of the energy to charged particles. Hopefully, the efficiency for such a process is at most a few percent, giving only a small correction to the counting rate.

De-excitation γ rays following muon capture are expected to be of the order of $\alpha = 1/137$ times as frequent as the neutrons, and also represent a correction of at most a few percent in the interval above 60 MeV.
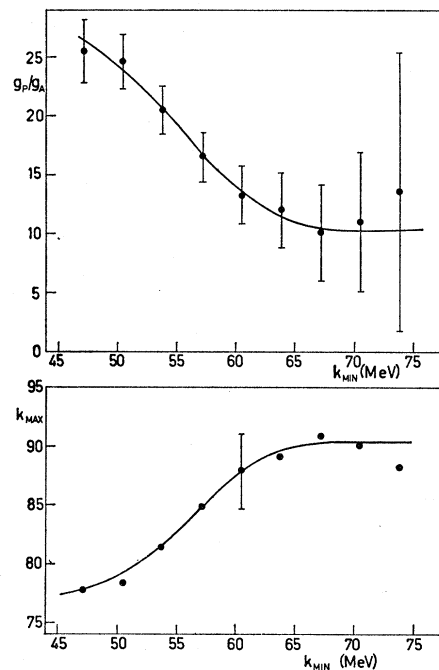

FIG. 9. The best-fit values of g_P and k_{max} as a function of k_{min}, the lowest energy of the data used in the fit. Except for g_P, the standard coupling constants were assumed for the fit. The errors shown for g_P are statistical only, and include the uncertainty in k_{max}. The points are not statistically independent, and care must be exercised when comparing neighboring points.

[42] L. Foldy (private communication).
[43] D. E. Hagge, University of California Radiation Laboratory Report UCRL-10516, 1963 (unpublished).

TABLE III. The results of least squares fitting the theoretical spectra to the data between 60 and 100 MeV; g_P^π (or Δg_P) and k_{max} were adjusted to give the best fit for each set of the coupling constants. The errors shown are statistical only. For all fits $g_T=0$.

g_A/g_V	g_M/g_V	g_S/g_V	Best fit for g_P^π/g_A or	$\Delta g_P/g_A$	Best fit for k_{max} (MeV)
−1.2	3.7	0	$\Big\{$ −34 ±7	0	87.7
			13.3±2.5	0	87.9
−1.0	3.7	0	14.3±2.7	0	87.9
−2.0	3.7	0	11.9±2.1	0	87.6
−1.2	0	0	11.7±2.2	0	87.8
−1.2	3.7	0	14.9±2.5[a]	0	82.3[a]
−1.2	3.7	0	8	10.4±5.6	88.6
−1.2	3.7	−1	8	6±5	88.8

[a] For this fit the energy calibration of the NaI counter was taken 6% lower than usual, as suggested as a possible explanation of the low-energy discrepancy.

These small corrections were not made because of the uncertainty in their estimate. As one proceeds to lower energies, however, such contaminations increase rapidly and may be the cause for the low-energy discrepancy discussed above.

Due to the uncertainty of the data below about 60 MeV, only the data above 60.4 MeV have been used in the fits which have been made to obtain information about the coupling constants. The points above 100 MeV were not used either. The results of several fits are shown in Table III. For each fit, all coupling constants but one were held fixed; the remaining coupling constant and k_{max} were varied to find the best fit. These fits are discussed in the next section.

V. THEORETICAL INTERPRETATION

Fits for g_P and k_{max} were obtained using the "standard" values for the other coupling constants (we use the notation of Luyten, Rood, and Tolhoek[44]):

g_V = vector coupling constant,

g_A = axial vector coupling constant = $-1.2g_V$,

g_M = weak magnetism coupling constant = $3.7g_V$,

g_S = scalar coupling constant = 0,

g_T = tensor coupling constant = 0.

The data are fitted well for two values of g_P:

$$g_P = -(34\text{−}\pm7)g_A, \qquad (11a)$$

and

$$g_P = (13.3\pm2.7)g_A. \qquad (11b)$$

The errors represent both the statistical uncertainty (including that of k_{max}) and a 10% systematic uncertainty, mainly for the effective solid angle.[45]

[44] J. R. Luyten, H. P. C. Rood, and H. A. Tolhoek, Nucl. Phys. 41, 236 (1963).
[45] If we exclude the data from the first half of run IIa (the data with an abnormally low counting rate), the best-fit result for g_P/g_A goes from 13 to 18, and that for k_{max} changes from 88 to 84 MeV.

The reason for obtaining two different possible values of g_P is shown qualitatively in Fig. 10a, where the theoretical value[16] of

$$I(x_{min}) = \int_{x_{min}}^{\infty} [N(x)/\Lambda_{\mu c}]dx, \qquad (12)$$

modified by the experimental resolution, is plotted as a function of g_P for $x_{min}=0.68$. The corresponding experimental value is just the normalized number of events above 60 MeV; this value is drawn as a band with width corresponding to the statistical uncertainty (including that in k_{max}). The experimental band intersects the curve in two places, giving two possible values for g_P. Using the results of other experiments,[24–29] we can reject the large negative solution; it is interesting to note that conversely, the results of this experiment can be used to exclude the "second solution" of the other experiments, namely, a very large positive value for g_P/g_A.

The best-fit value of g_P is not very sensitive to variations in g_A and g_M, as suggested by Fig. 1 and shown by Table III. There is also not much dependence of g_P on the energy calibration; a change in calibration of -6% (the calibration suggested as a possible explanation of the excess of events at low energies) changes g_P from $13.3g_A$ to $14.9g_A$.
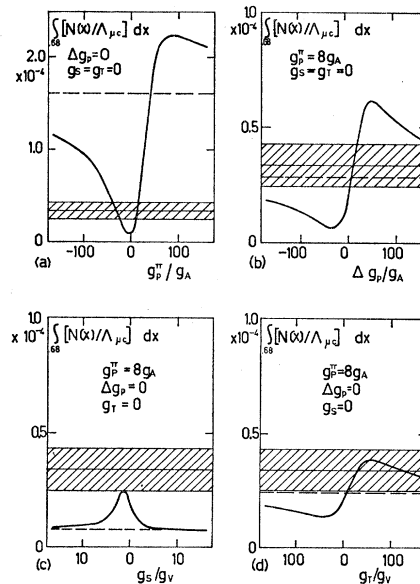

FIG. 10. The integral of the theoretical spectrum (spread by NaI counter resolution) from $x=0.68$ up; this lower limit corresponds to 60 MeV for $k_{max}=88$ MeV. The curves are drawn for $g_A/g_V = -1.2$, $g_M/g_V=3.7$, and the other coupling constants as stated in the figure. For large positive and negative values of the variable coupling constants, the curves approach the asymptotic limits shown as dotted lines. The experimentally determined value ±one standard deviation (including the uncertainty in k_{max}) is shown as the shaded band.

The best-fit value for k_{max} is

$$k_{max} = 88 \pm 4 \text{ MeV}. \tag{13}$$

As shown in Table III, it is relatively independent of the values chosen for the coupling constants held fixed; changing the energy calibration, however, changes the apparent value of k_{max} by a proportionate amount. The average excitation energy given to the residual K^{40} nucleus corresponding to the above value of k_{max} is

$$\bar{\epsilon} = 15 \pm 4 \text{ MeV}. \tag{14}$$

Using the theory of Rood and Tolhoek[16] to extrapolate the experimental data to low photon energies, we obtain for the branching ratio of radiative to ordinary muon capture in Ca^{40}:

$$R = (3.1 \pm 0.6) \times 10^{-4}. \tag{15}$$

For all the fits shown in Table III, χ^2 was about 18.5 for 23 degrees of freedom, giving $P_{\chi^2} = 70\%$.

The discrepancy between our experimental result for g_P/g_A and the theoretical prediction[20] of about 8 is two standard deviations; this may, of course, be simply the result of a statistical fluctuation. It may also be due to inadequacies of the theory which was used to deduce g_P from the photon spectrum. For example, in a complex nucleus the radiative capture process might be appreciably affected by pionic exchange currents between nucleons, and by the fact that the terms corresponding to the diagrams of Fig. 2 may be altered by the pion propagating in nuclear matter. Such effects are expected to depend on the mass number A of the nucleus involved, and one might eventually hope to see their relative importance by comparing the present experiment with a similar one using O^{16} as the capturing medium.

Although statistical and theoretical uncertainties could account for the large counting rate of our experiment, it is amusing to investigate other possible explanations. For example, Wolfenstein[46] has suggested that the pseudoscalar coupling be divided into two terms:

$$g_P(q^2) = g_{P^{\pi}} \frac{m_{\pi}^2 + m_{\mu}^2}{m_{\pi}^2 + q^2} + \Delta g_P, \tag{16}$$

where q^2 is the pion four-momentum transfer squared, $g_{P^{\pi}} \approx 8g_A$ is the strength of the one-pion-exchange contribution,[47] and Δg_P takes into account other contributions, presumably associated with pseudoscalar objects much heavier than the muon,[47a] and thus having

only a small dependence on $|q^2| \leq m_{\mu}^2$. For ordinary capture, $q^2 \approx m_{\mu}^2$ and Eq. (16) becomes

$$g_P \approx g_{P^{\pi}} + \Delta g_P, \tag{16'}$$

whereas for our experiment, q^2 may also be negative and, averaging over the photon spectrum from 60 MeV up and comparing with Eq. (11b), we effectively obtain

$$g_P \approx 2g_{P^{\pi}} + \Delta g_P \approx 26g_A. \tag{16''}$$

Fixing $g_{P^{\pi}} = 8g_A$ and using Δg_P and k_{max} as variables, our fitting procedure yields

$$\Delta g_P = (10.4 \pm 5.6) g_A, \tag{17}$$

where the systematic and statistical errors are shown. This value for Δg_P corresponds to $g_P \approx 18g_A$ for ordinary muon capture experiments. As is shown in Fig. 10(b) there are also two other mathematical solutions which presumably have nothing to do with reality, namely, very large positive or negative Δg_P. In principle, our experiment could be combined with an ordinary capture experiment to give $g_{P^{\pi}}$ and Δg_P; but the experimental and theoretical uncertainties are at present several times too large for this to be meaningful.

Another possible interpretation of our large counting rate is that the scalar and/or tensor terms are important. Strangeness-conserving vector currents may be split into two distinct classes according to their transformation properties under G parity.[48] The scalar and the tensor terms belong to the so-called "second class." They are generally taken to be zero,[44] so that the weak currents may have definite transformation properties under G-parity transformation. The conserved vector current hypothesis implies that the vector current has no second-class term, i.e., $g_s = 0$. On the other hand, no definite evidence exists at present against second-class terms in the axial vector current, even though only first-class terms are allowed if the weak bare couplings are simply V and A. The contribution of a possible second-class axial vector current to radiative muon capture has been examined recently by Borchi and Gatto.[49] Such a contribution leads to a tensor term with coupling constant g_T which can be fit to our data. Setting the other coupling constants to their "standard" values (including $g_{P^{\pi}} = 8g_A$ and $\Delta g_P = 0$) and adjusting g_T and k_{max} gives reasonable agreement between theory[16] and data for

$$g_T \gtrsim 15g_V, \tag{18}$$

as can be seen from Fig. 10(d). Investigations of the ft values of beta transitions from the mirror nuclei B^{12} and N^{12} have also been interpreted in terms of a tensor coupling.[50]

For completeness, we have also fit the data by varying g_s. As can be seen in Fig. 10(c), the theory[16] (with the

[46] L. Wolfenstein, *International Conference on Fundamental Aspects of Weak Interactions* (Brookhaven National Laboratory, Upton, New York, 1963); p. 292; also private communication.

[47] In the fits discussed previously, we have been quoting the values obtained for $g_{P^{\pi}}$ with $\Delta g_P = 0$.

[47a] *Note added in proof.* In a recent theoretical work by J. C. Taylor [Phys. Letters **11**, 77 (1964)] it has been shown that contributions due to exchange of masses higher than the pion mass are of only a few percent.

[48] S. Weinberg, Phys. Rev. **112**, 1375 (1958).

[49] G. Borchi and R. Gatto (to be published).

[50] J. N. Huffaker and E. Greuling, Phys. Rev. **132**, 739 (1963).

other coupling constants fixed at their "standard" values) gives a fair fit in the neighborhood of $g_S = -1.3g_V$.

We stress that the value of these speculations is limited by the theoretical and experimental uncertainties mentioned above.

VI. COMPARISON WITH OTHER EXPERIMENTS

Our ratio of radiative to ordinary muon capture in Ca^{40} has, within the errors, the same value reported for the case of copper by the Chu et al.[2] However, these results differ from those of the previous CERN experiment,[1] in which 10 ± 4 events with $k>60$ MeV were observed in iron, compared with 22 events predicted by normalizing our data to the conditions of that experiment.

The value of g_P obtained by the present experiment can be compared with the values derived by various experimental investigations of ordinary muon capture. The rate of μ^- capture in liquid hydrogen has been measured by a number of groups[24] and is consistently found to be about 20% lower than predicted theoretically with the "standard" coupling constants. There are a number of possible explanations[23,24] for this discrepancy; in particular, the calculated molecular wave-function overlap could be in error by 10%, or one or more of the coupling constants could be different from that normally assumed. If the discrepancy were due only to g_P/g_A being unequal to eight, a value $g_P/g_A = 15.5\pm3.5$ is obtained, in agreement, within the errors, with the results of the present experiment. (It is interesting to note that such a discrepancy can be interpreted also with $g_P \approx 8g_A$ and $g_T \approx 15g_V$.)

The difficulties which prevent an unambiguous interpretation of μ^- capture in hydrogen do not arise for the process $\mu^- + He^3 \rightarrow He^3 + \nu$, the rate of which has been measured by various authors[25] and is now known to within a 3% error. These measurements have been recently interpreted[51-53] in terms of the induced pseudoscalar interaction. The He^3 capture rate, however, is only moderately sensitive to g_P/g_A in the region of interest; going from 8 to 16, the expected rate reduces by only 9%, compared with a 5 to 10% theoretical uncertainty. The value of g_P obtained by our experiment is not inconsistent with these results.

Muon capture by C^{12} leading to B^{12} in its ground state provides another, although not very sensitive, method of determining the constant g_P. The latest experiments on this process give results which are consistent with both the value of g_P predicted theoretically and the values of g_P obtained by our experiment.[29]

Measurements have also been made, at Columbia and more recently at Berkeley, of the O^{16} partial muon capture rates.[26] In particular, the partial rates for

transitions leading to the 0^- and 2^- states of N^{16} are strongly dependent[27] on the value of g_P. The interpretation of these experiments is made difficult by insufficient knowledge of the wave functions involved. A more detailed analysis of the Columbia data on the 0^- transition has resulted in a shift of the value of g_P/g_A from 15 (as originally reported) down to the present value of 5 to 10. The Berkeley 0^- results indicate that g_P/g_A lies between 0 and 8. However, it seems that the 2 rate measured by the Columbia group cannot be explained with the usual values of g_V, g_A, and g_M; it suggests a very large value for $g_P/g_A (\gtrsim 16)$.

A very large value of g_P/g_A is also indicated by recent measurements[28] at Dubna on the angular distribution of neutrons following the capture of polarized muons in Ca^{40}. In this experiment, the asymmetry parameter is found to be -1 ± 0.15 for neutrons with energy greater than 19 MeV. This rather surprising result suggests a value of $g_P \approx 30g_A$, but cannot be satisfactorily explained for any value of g_P unless at least one other coupling constant is changed. It is suggested that in addition to $g_P \approx 30g_A$, either[28] $g_A = -(2$ or $3)g_V$, or[54] $g_S = -g_V$. As shown by Table III, using these coupling constants with our data gives values for g_P which are in marginal agreement with the asymmetry experiment.

It is also interesting to compare with other experiments our result of (15 ± 4) MeV for the average excitation energy given to the product nucleus K^{40} by the radiative muon capture process. Hagge[43] has studied the neutron energy spectrum from ordinary capture in Ca^{40} and finds a nuclear excitation of (13 ± 2) MeV, which does not differ significantly from our result.

In order to explain the discrepancy between observed and expected muon capture rates in O^{16}, Barlow et al.[55] suggest that this process leads to giant resonance formation in the product nucleus.[56] If this were the case for radiative capture in $Ca,^{40}$ one would expect an excitation energy of about 13 MeV, which also compares favorably with our measured value.

VII. CONCLUSIONS

Using the "standard" values for the other coupling constants, we get good agreement between the theory of Rood and Tolhoek[16] and the experimental data for

$$g_P = (13.3\pm2.7)g_A, \qquad (11b)$$

$$k_{max} = 88\pm4 \text{ MeV.} \qquad (13)$$

Using the theory to extrapolate the experimental spectrum to low γ-ray energies gives the ratio of radiative to ordinary capture as

$$R = (3.1\pm0.6)\times10^{-4}. \qquad (15)$$

[51] W. Dreschler and B. Stech, Z. Physik 178, 1 (1964).
[52] A. Fujii and Y. Yamagouchi, Progr. Theoret. Phys. (Kyoto) 31, 107 (1964).
[53] A. F. Yano, Phys. Rev. Letters 12, 110 (1964).

[54] M. L. Yovnovich and V. S. Evseev, Phys. Letters 6, 333 (1963).
[55] J. Barlow, J. C. Sens, P. J. Duke, and M. A. R. Kemp, Phys. Letters 9, 84 (1964).
[56] L. Foldy and D. Walecka, Nuovo Cimento (to be published).

The above value of k_{max} corresponds to an average excitation energy given the K⁴⁰ residual nucleus of

$$\bar{\epsilon} = 15 + 4 \text{ MeV}. \quad (14)$$

The errors given to these quantities correspond to the statistical and systematic uncertainties only; no theoretical uncertainty has been included.

The value for g_P given above is about two standard deviations larger than the theoretically expected value of (7 or 8)g_A. This discrepancy may of course be only a statistical fluctuation; it may also be due to inadequacies of the theory used to correlate the experimental spectrum to values of the coupling constants.

Various other experiments[24,28] also suggest large values for g_P. If g_P really were larger than the (7 or 8)g_A predicted theoretically for one-pion exchange, then we should perhaps assume that the excess Δg_P has little or no dependence on the momentum transfer, unlike the one-pion-exchange term.

Our data then give

$$\Delta g_P = (10.4 \pm 5.6)g_A. \quad (17)$$

An alternative explanation for our large counting rate can be obtained by allowing the axial-vector part of the weak nucleonic current to not have a definite G-parity. Reasonable fits to the data can then be obtained using the "standard" coupling constants, but with a tensor term having

$$g_T \gtrsim 15 g_V. \quad (18)$$

Further experimental work is needed to establish whether nuclear effects are responsible for the large value of g_P obtained by the present experiment; in particular, an investigation of the radiative muon capture process in O¹⁶ (which is also a double closed-shell nucleus) could hopefully throw light on this point. Other interesting experiments remain to be done on radiative muon capture; for example, the measurement of the angular distribution of γ rays emitted when polarized muons are captured in Ca.⁴⁰ Although this experiment would not be sensitive to g_P, it would be extremely sensitive to whether or not the interaction were V, A, or S, T. Eventually, one might hope that with improved techniques it will also be possible to study the most interesting process of radiative muon capture in hydrogen.

ACKNOWLEDGMENTS

APPENDIX

The energy loss of electrons by ionization was needed both for the energy calibration of the NaI crystal and for the contamination corrections. This quantity is not tabulated for $E \gtrsim 10$ MeV, since energy loss by bremsstrahlung plays an important role; in our case, however, the bremsstrahlung radiation (emitted essentially forward) is in general detected by the NaI crystal.

For this reason, an experimental determination of the energy loss by ionization was made. The NaI crystal was used to detect shifts in the upper edge of the μ^+-decay electron spectrum when varying thicknesses of material were interposed between the electron source and the crystal. Both the experimental arrangement and the analysis were quite similar to those used for the NaI energy calibration. The results gave the ionization energy loss for positrons of ~ 45 MeV as

$$\left(\frac{dE}{dx}\right)_{Ca} = (1.65 \pm 0.09)\frac{\text{MeV}}{\text{g/cm}^2},$$

$$\left(\frac{dE}{dx}\right)_{CH} = (1.88 \pm 0.12)\frac{\text{MeV}}{\text{g/cm}^2}.$$

These values were increased by approximately 3% to obtain the rate of energy loss for negative electrons needed for the calculations.